NON-LINEAR FINITE-ELEMENT MODELLING OF ROOM AND PILLAR MINE WORKINGS INCLUDING THE STRAIN-SOFTENING BEHAVIOUR OF THE ROCK MASS

SALIM BENSEHAMDI and ABDELBAKI SERIANI

About the authors

Salim Bensehamdi
University Badji Mokhtar,
Faculty of Earth Science,
Mining Engineering Department
Bp 12 (23000) Annaba, Algeria
E-mail: seriani7@yahoo.fr

Abdelbaki Seriani
University Badji Mokhtar,
Faculty of Earth Science,
Mining Engineering Department
Bp 12 (23000) Annaba, Algeria
E-mail: seriani7@yahoo.fr

Abstract

A two-dimensional model adopting post-failure criteria was used to simulate the behaviour of the rock mass and the development of yield zones around room and pillar mine workings. The model conformed to the strain-softening behaviour of the rock mass and accounted for its post-failure residual strength. The structural-stability-analysis approach accounted for the main features of the mine structures' yield produced during loading through changes in the rock material's stiffness and the subsequent evolution of the stresses. A comprehensive parametric analysis was performed and the inevitable effect of the interaction of the roof, pillar and floor on the overall stability limit of the mine was investigated. The numerical results clearly showed that the finite-element linear models could not realistically represent the true behaviour of the mine structure. However, they clearly demonstrated the limitations of the finite-element linear solutions in representing the true behaviour of the mine structure, particularly when the rock-mass structure is relatively weak, and that a non-linear approach was justified.

Keywords

non-linear FE analysis, yielding, plastic zones, room and pillar mining, residual strenght, stability assessment

1 INTRODUCTION

One of the most difficult design problems in practical rock mechanics arises in conditions of the rock mass's complex non-linear constitutive behaviour, including structural discontinuities, and the non-homogeneity of the medium [7]. Field measurements and laboratory tests have shown the presence of the strain-weakening behaviour of the rock mass and have indicated that in many cases the assumption that the rock is linearly elastic leads to calculated stresses and displacements that disagree significantly with the measured values. In particular, as the rock mass around an excavation may exist in the post-yield state [2], [3], a realistic approach should incorporate the effect of the post-yield behaviour in the analysis [5], [10]. In the current finite-element analysis this has usually been achieved by adopting an elastic, perfectly plastic model and gradually changing the material coefficients of the yielding materials using a quasi-elastic finite-element solution [4]. In this paper an advanced elastic-plastic LUSAS finite-element program [6] was used to predict the distribution of stresses during the plastic and elastic strain states, and to simulate the possible mechanisms of the yield of the rock mass around a mine opening. This accounted for the residual strength after the failure.

2 DESCRIPTION OF THE MATERIAL MODEL

The solutions of existing non-linear material models that are used to simulate rock mechanics and other geotechnical problems are somewhat limited in their ability to properly reflect the behaviour of the complete stress-strain curve of most rock materials. [5] Both laboratory and field measurements have indicated that immediately after the peak strength level is reached, the stress-strain curve drops with a negative gradient and then flattens out at a residual strength. The classical solution adopting the constant-load incremental technique has been shown to fail when the solution reaches the limit points

on the material stress-strain curve, as shown in Fig. 1 and Fig. 2, [4], where either load- or displacement reversal occurs, resulting in a singular stiffness matrix, which automatically leads to the failure of the solution to converge. The LUSAS finite-element programs [6] used in this analysis contain a model that allows a simulation of the material's behaviour well into the strain-softening part of the stress-strain curve.

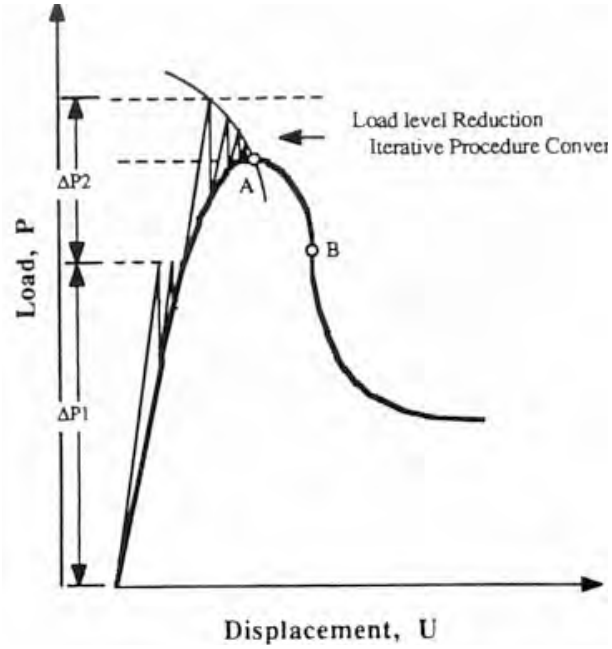

Figure 1. LUSAS modified arc length incrementation solution.

A general method that may follow the solution path through the well-known post-peak portion of the material's stress-strain curve is the modified arc-length technique [1]. The salient characteristic of the arc-length technique is that the load level does not remain constant at each load increment, where during each iteration the load level is modified so that convergence near the limit points A and B can be achieved, Fig. 1. A typical, modelled, material stress-strain characteristic is illustrated in Fig. 2, where the complete stress-strain curve of the tested rock material is matched by a series of elastic and plastic lines, K_0, K_1, and K_n, corresponding to the material's performance in the elastic and plastic states [5].

The initial portion of the model, as matched by the plastic line k_1, represents the work-hardening behaviour of the material, which is characterized by increasing stress with plastic deformation, while the second portion of the model shows the behaviour of the strain-softening state of the material, having a residual strength that decreases with plastic deformation, and finally an ideally plastic state of the material, where the deformation increases at constant stress.

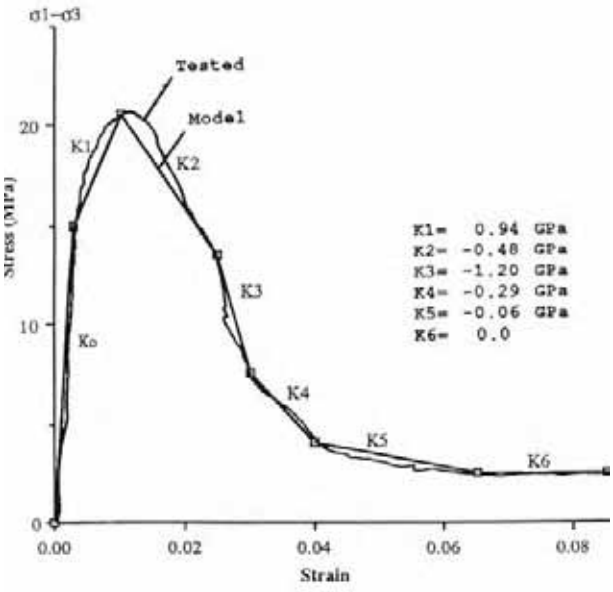

Figure 2. Modelled material stress-strain curve.

3 CONSTITUTIVE LAW

In the elastic range, the way in which the stress and the strain are related for a material under load is described qualitatively by its constitutive behaviour. For an isotropic body undergoing plane-strain deformation, the stress-strain relation follows Hooke's law Eq. (1), that is:

$$\{\sigma\}_e = [\mathrm{E}]_e \{\varepsilon\}_e$$

$$\{\sigma\}_e = \begin{vmatrix} \sigma_x \\ \sigma_y \\ \sigma_z \end{vmatrix}, \{\varepsilon\}_e = \begin{vmatrix} \varepsilon_x \\ \varepsilon_y \\ \varepsilon_z \end{vmatrix} \qquad (1)$$

$$[\mathrm{E}]_e = \frac{(1-\nu)}{(1+\nu)(1-2\nu)} \begin{vmatrix} 1 & \frac{\nu}{1-\nu} & 0 \\ \frac{\nu}{1-\nu} & 1 & 0 \\ 0 & 0 & \frac{1-2\nu}{2(1-\nu)} \end{vmatrix}$$

For non-linear material behaviour the plastic state is specified by:

1. A yield function to specify the onset of plastic deformation, Eq. (2):

$$\mathrm{F}(\{\sigma\},|\mathrm{K}|)=0 \qquad (2)$$

where

F: Yield function
{σ}: Stress vector
|K|: Hardening, softening parameter

In classical plasticity, stress states that provide a positive value of the yield function cannot exist. However, in numerical models, positive values of the yield function indicate that yielding should occur and the stress state is modified by accumulating plastic strains until the yield criterion is reduced to zero. This process is known as the plastic-corrector phase or return mapping.

2. A flow rule to define the plastic straining is given by Eq. (3):

$$\delta\{\varepsilon\}_{\mathrm{p}} = \lambda \frac{\partial \mathrm{F}}{\partial\{\sigma\}} \qquad (3)$$

where

$\delta\{\varepsilon\}_{\mathrm{p}}$: Increment vector of the plastic strain
$\frac{\partial \mathrm{F}}{\partial\{\sigma\}}$: Direction of the plastic strain
λ: Lagrangian plastic multiplier defining the magnitude of the plastic strain

3. A hardening and softening rule to define the evolution of the yield surface with plastic strain. This is defined by describing the evolution of the yield function in relation to the effective plastic strain, ε_{effp}, using a series of straight-line segments, Fig.2.

$$\mathrm{K}_{\mathrm{effp}} = \sigma_{\mathrm{y}} + |\mathrm{K}_{\mathrm{n}}|.\varepsilon_{\mathrm{effp}} \qquad (4)$$

where

$\mathrm{K}_{\mathrm{effp}}$: Effective hardening, softening slope
σ_Y: Initial yield stress
$|\mathrm{K}_{\mathrm{n}}|$: Hardening, softening slopes

During an increment of stress, δ(σ), changes in the strain are assumed to be the sum of an elastic and a plastic component. Thus, the concept of total strain will be invoked, Eq. (5):

$$\delta\{\varepsilon\} = \delta\{\varepsilon\}_{\mathrm{e}} + \delta\{\varepsilon\}_{\mathrm{p}} \qquad (5)$$

The elastic strain components, $\delta(\varepsilon)_{\mathrm{e}}$, are related to the stress components by a matrix of constant [E], known as the stiffness matrix Eq. (6):

$$\delta\{\varepsilon\}_{\mathrm{e}} = [\mathrm{E}]^{-1}.\delta\{\varepsilon\} \qquad (6)$$

Taking account of the elastic and plastic components produces Eq. (7):

$$\delta\{\varepsilon\}_{\mathrm{e}} = [\mathrm{E}]^{-1}.\delta\{\varepsilon\} + \lambda \frac{\partial \mathrm{F}}{\partial\{\sigma\}} \qquad (7)$$

The elastic-plastic stress and strain increments may be related by the following equation. Eq. (8):

$$\delta\{\varepsilon\}_{e} = [E]_{ep}.\delta\{\varepsilon\} \qquad (8)$$

where

$[E]_{\mathrm{ep}}$ is the elasto-plastic stiffness matrix

During the elastic-plastic analysis, the material's stiffness matrix is updated by the new, computed elastic-plastic stiffness matrix, $[E]_{ep}$, at each increment of the finite-element solution [2], [3].

4 THE NON-LINEAR FINITE-ELEMENT TECHNIQUE

The technique for performing a non-linear finite-element analysis is illustrated in Fig. 3 (next page).

This technique is summarized as follows:

1) First, load increments are applied to the mine structure and the strains and hence the stresses are found at the Gaussian points in the elements. For each increment of load, an initial material stiffness is used and the elastic solution is obtained.

2) During the solution the courses of all the finite elements are checked for yield. If the stresses at the Gaussian points lie within the previously prescribed yield surface, the stress update has been completed. Otherwise, stress lying outside the yield surface must be returned to the yield surface by plastic straining. During each iteration cycle, computed stresses and strains are added to the total already accumulated and a new material-stiffness matrix is reformulated for the next load increment. Within each load increment the system of Eq. (9):

$$\delta\{\sigma\}_{i} = [E]_{iep}.\delta\{\varepsilon\}_{i} \qquad (9)$$

must be solved for the strain increment $\delta\{\varepsilon\}_{i}$

where

δ{σ}i : Increment of stress during iteration, i
$[E]_{iep}$: Updated elasto-plastic stiffness matrix
$\delta\{\varepsilon\}_{i}$: Strain increment during iteration
$\delta\{\varepsilon\}_{i} = \left(\delta\{\varepsilon\}_{e} + \delta\{\varepsilon\}_{p}\right)$

3) Steps (1) and (2) are repeated for all the increments of load that constitute the total load applied to the structure.

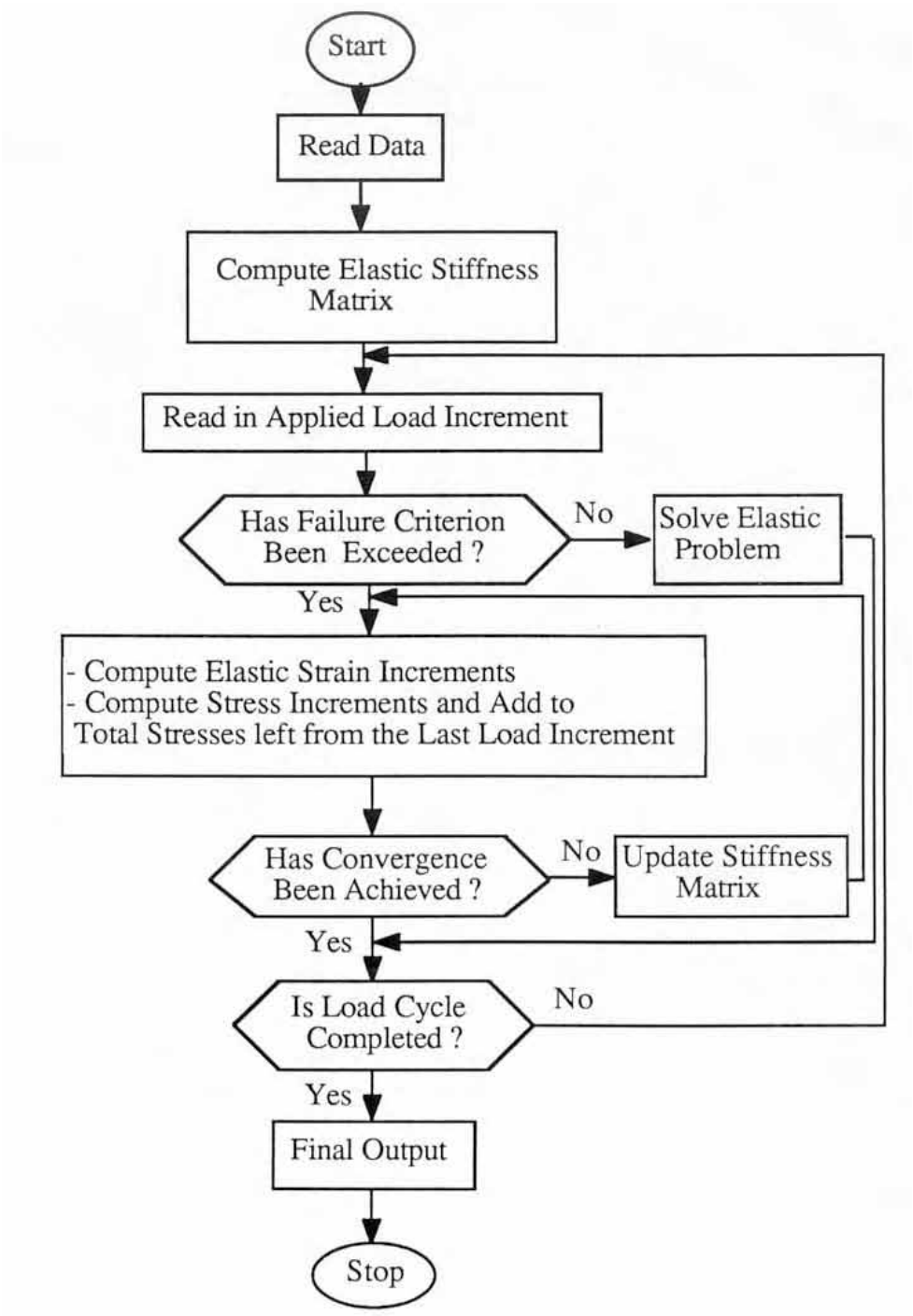

Figure 3. Simplified plasticity-solution flow diagram.

5 TWO-DIMENSIONAL FINITE-ELEMENT ANALYSIS OF ROOM AND PILLAR MINING

5.1 BOUNDARY CONDITION OF THE PROBLEM

A two-dimensional finite-element model under plane strain of a typical room and pillar mine working is illustrated in Fig. 4.

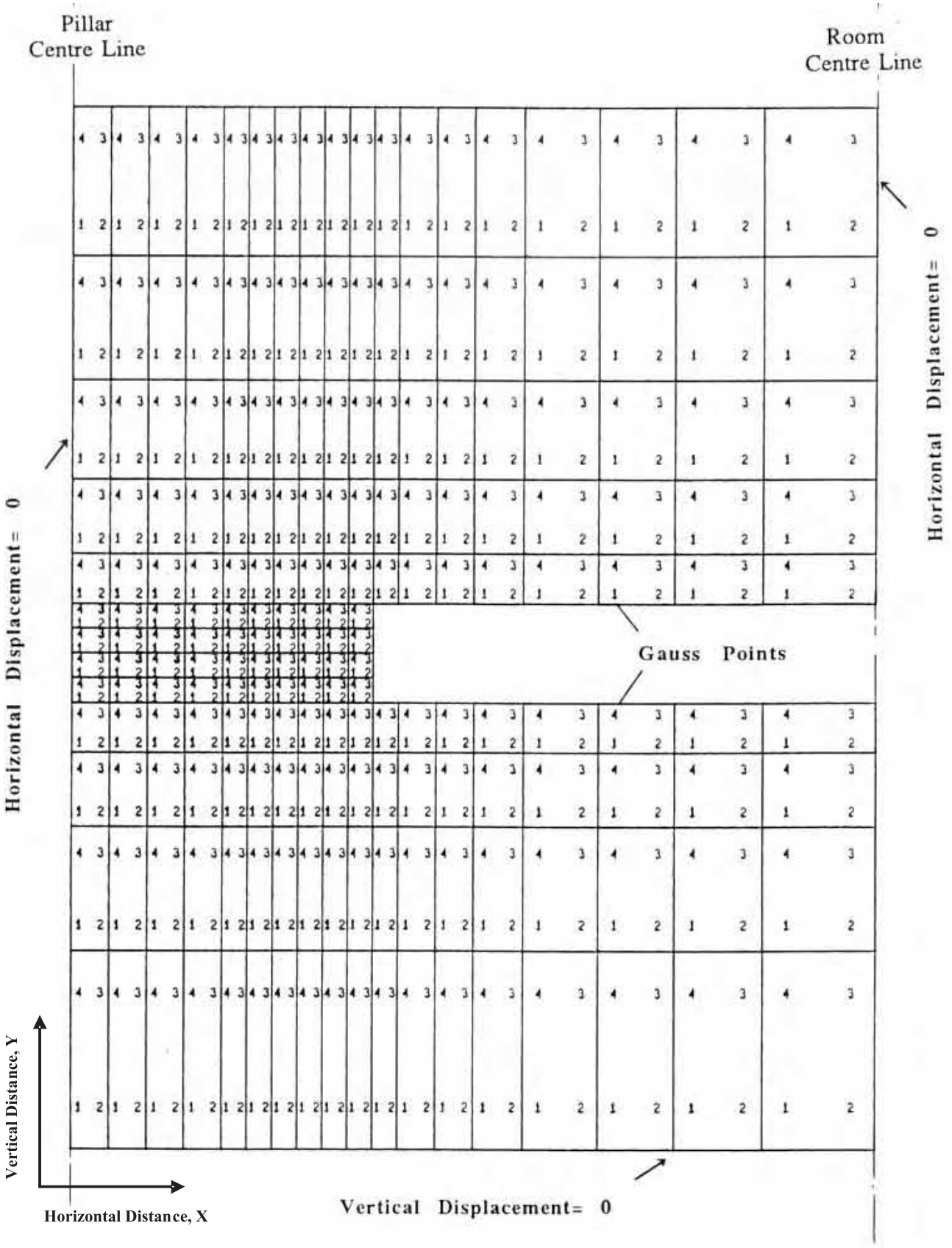

Figure 4. Typical finite-element mesh of room and pillar mining configuration of vertical cross-section with boundary conditions.

The model consists of 202 four-noded isoparametric elements. Since the mesh of the model was symmetrical, only half of the configuration was considered. Lateral movement in the X direction of the model was prevented on its sides, allowing only vertical movement in the Y direction to occur. The nodal points corresponding to the lower strata of the floor were held fixed in both directions. The model enabled different mining configurations to be simulated with various properties, as well as the stress-strain behaviour to be assigned to the roof, pillar, and floor, Table. 1

point is readjusted and the elements' post-yield stiffness is updated according to the criterion of the stress and strain-softening laws, respectively. The stress around the entry is then redistributed and shifted to the unyielding or stiffer parts of the structure, as the surrounding rock mass seeks the final equilibrium steady state under a given overburdened load and mining sequence.

The structural stability analysis is first focused on the assessment of the overall stability of the support pillars in terms of the maximum yield that occurs throughout

Table 1. Physical and mechanical properties of the model strata.

Model strata sequence	Material type	Young's modulus E, MPa	Unit Weight γ, Kg/m^3	Poisson's ratio υ	Uniaxial Compressive Strength, σ_c, MPa	Shear strength τ_c, MPa	Friction Angle φ, (°)
Roof	Marl - Limestone	20000	2550	0.20	20.0	7.0	45
Immediate roof	Marl	3000	2600	0.35	12.0	2.0	35
Pillar	Coal	3600	2500	0.35	20.6	0.5	33
Immediate floor	Organic Marl	3300	2500	0.40	2.8	1.8	30
Floor	Limestone	15000	2500	0.25	35.0	6.0	34

5.2 FINITE-ELEMENT METHOD

Quite frequently, the only information required from the designer is that of determining the mine-structure collapse situation. It has been shown that under stiff loading, the progressive failure of rocks in compression is associated with a decrease in strength through accumulated plastic deformation and fracture. The inelastic post-yield characteristics of the rock strata are the major variables that characterize the mechanical behaviour of the yielded rock material in the post-failure state. The relationship between post-failure strength and stiffness is established according to a given material failure criterion and is used to simulate the growth of the yield zone surrounding a mine opening and hence to assess its overall stability.

In the following structural stability analysis of room and pillar mine workings a non-linear finite-element analysis is performed, adopting the Mohr-Coulomb yield criteria. The model simulates the behaviour of a mine structure in two stages: an elastic state prior to yielding, followed by a plastic state for the strain-weakening behaviour of the rock material. The plastic incremental analysis takes into consideration the degree of local yielding that occurs around the mine opening. Through a series of successive computer runs, all the Gaussian points are checked against failure, and if any violation of the stress criterion is detected then the stress state at the Gaussian

the pillar's cross-section [8], [9]. The extent and development of the yield zone through the pillar's width can be compared to the remaining elastic core of the effective support that the pillar still retains after yield. Under small loads, only a minor yield portion of the pillar rib develops.

However, if the pillar is loaded to such a degree that the yield zone extends throughout the whole cross-section of the pillar, then the oveall instability of the pillar occurs.

6 RESULTS OF THE FINITE-ELEMENT ANALYSES

A series of elastic-plastic finite-element runs was first performed under plain-strain conditions for the purpose of estimating the changes to, and location of, the peak abutment stress in the pillar as it yields progressively under loading. Fig. 5 shows the evolution of the finite-element-computed vertical stress component stresses for a complete loading cycle under plastic conditions, compared to the computed vertical stress components that could have arisen under purely elastic conditions. The total load on the pillar was initially applied in small increments so as to simulate the behaviour of a pillar during the transition from the elastic to the plastic state. As the load is applied, the pillar progresses through two

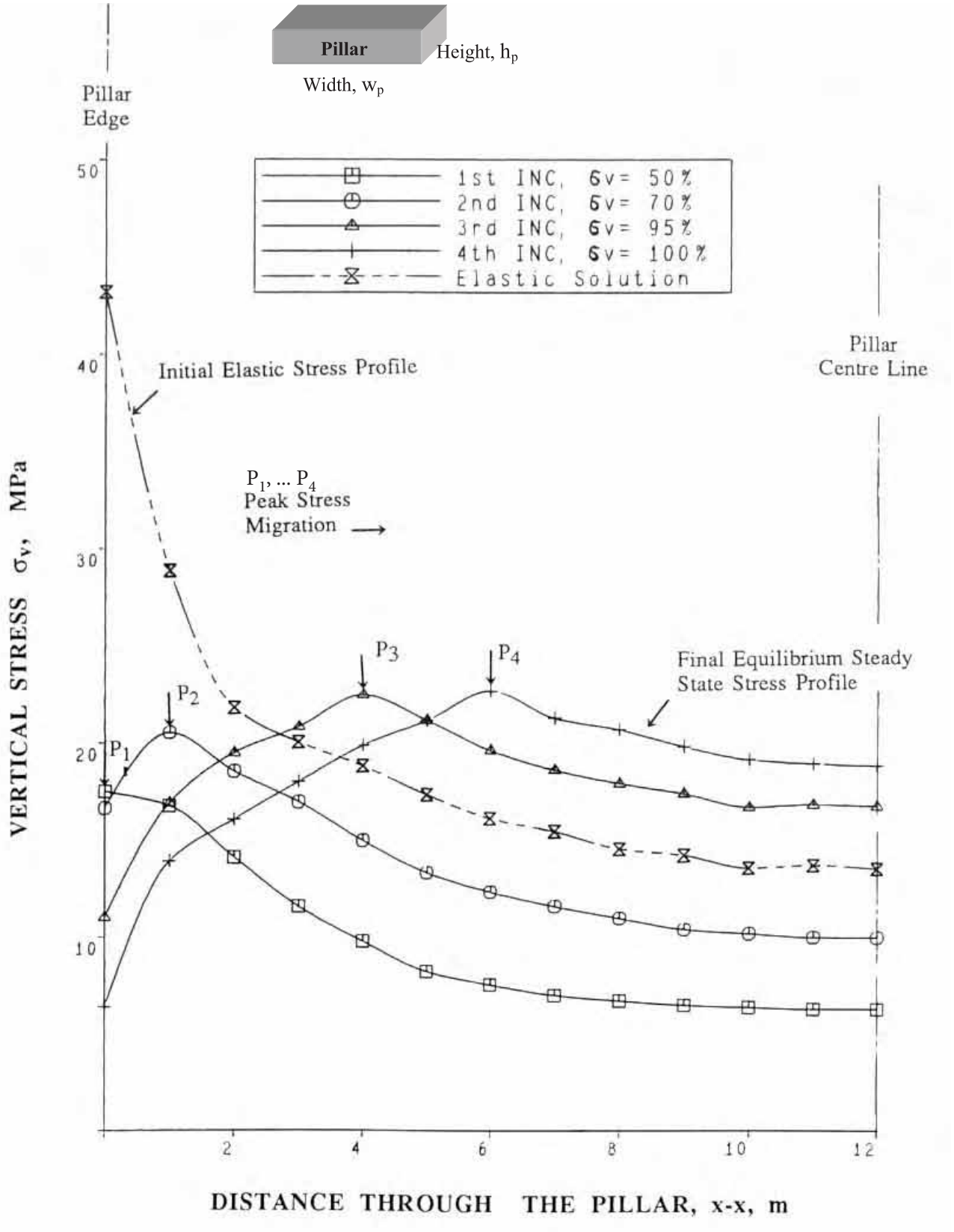

Figure 5. Change in the vertical stress profile in a yielding support pillar, extraction ratio r = 60%, w_p/h_p = 6.0.

distinct stages: an elastic deformation and yield work hardening, which is maintained up to the pillar material's bearing strength of 20.6 MPa, Fig. 2, and the collapse of the mine structure, which is represented by yield work softening. During the yielding process, the pillar material loses its bearing strength, with the excess of the stress being absorbed by the plastic deformation. The peak load built up on the pillar P_1, … P_n, Fig. 5, is then shifted towards the pillar core as the yield progresses. However, the yielded parts of the pillar still develop some bearing strength, but this depends on the post-yield material's properties, the magnitude of the applied load and the distance from the previously yielded part of the pillar. A good representation of this stress-change phenomenon is clearly illustrated in Fig. 5, where a significant difference in the vertical stress prediction

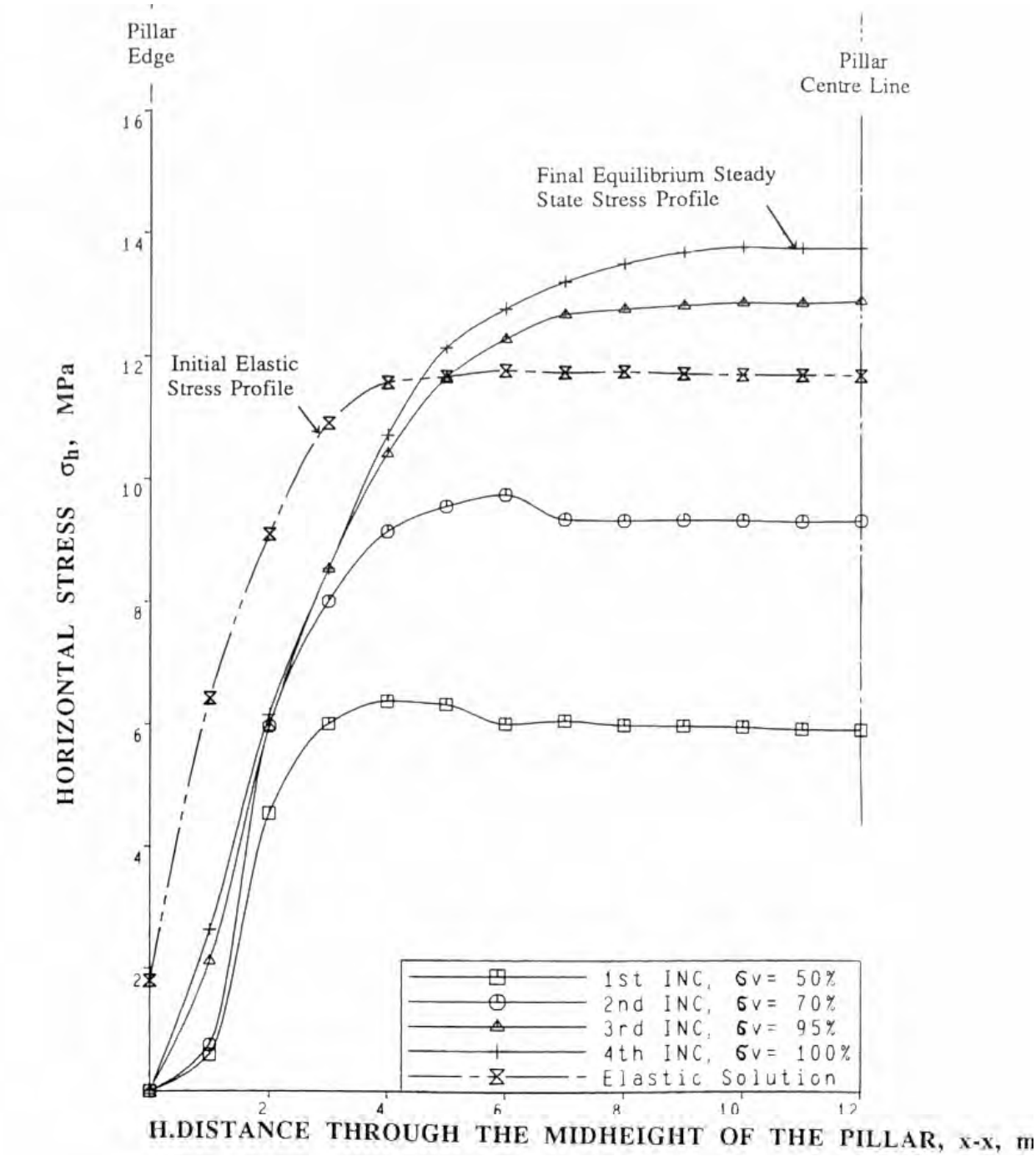

Figure 6. Change in the horizontal stress profile in a yielding support pillar, extraction ratio r = 60%, w_p/h_p = 6.0.

has been found when compared to the final steady-state stress profile predicted from the plastic solution and that predicted from the elastic one.

The induced horizontal stress components at the mid-height of the pillar for various increments of the applied load are given in Fig. 6, where theses stress components are seen to increase from zero at the pillar edge to a maximum value at the centre of the pillar.

Vertical and horizontal stress contour plots for yielding roof, pillar and floor are given in Fig. 7.

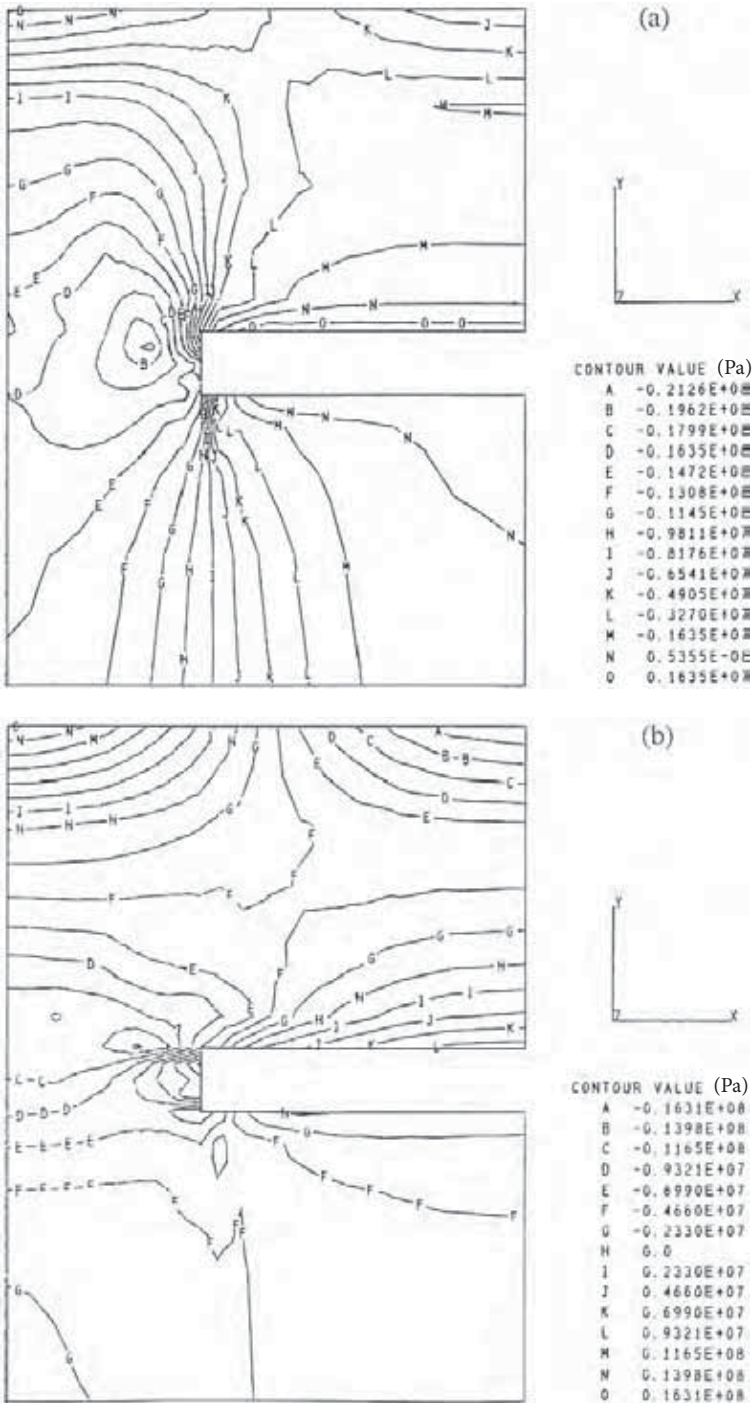

Figure 7. Vertical and horizontal principal stress contours, a and b, in a yielding room and pillar mine structure at the final equilibrium steady state.

The plots provide an excellent picture of the final state of the induced stresses of the yielding mine structure, which shows stress-relief zones around the pillar corners and some distance into the mine structure, where the peak stress is built up.

The shear-stress contours given in Fig. 8b show a shear-stress concentration at the roof-pillar intersection given by an elastic FE solution, while in Fig. 8a the shear stress is seen to be much lower in this area, and the reduced peak shear stress is shifted vertically in the roof.

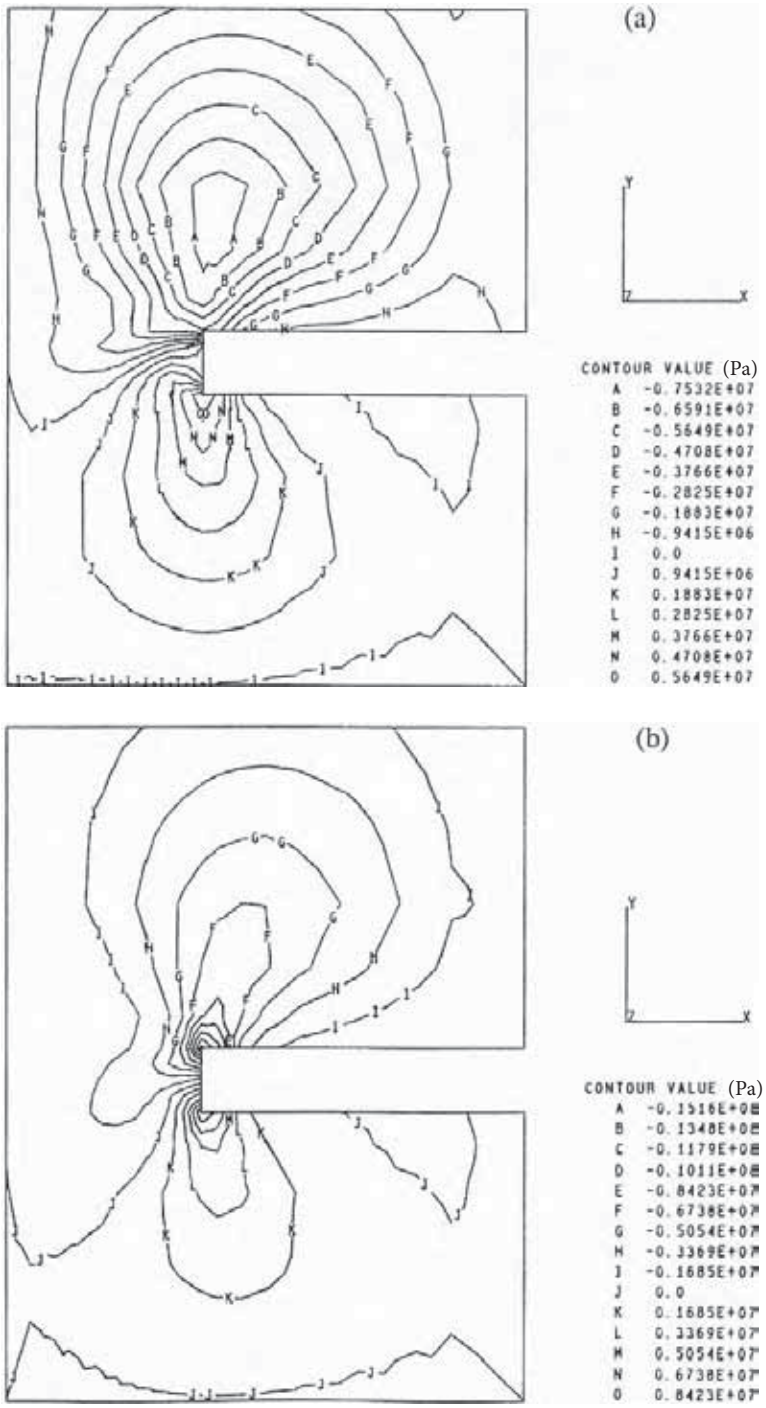

Figure 8. Shear-stress contours in a yielding plastic FE solution (a), and unyielded elastic FE solution (b), of a room and pillar mine structure at the final equilibrium steady state.

A relationship exists between the yield deformations of the pillar, where three distinct stress zones develop as the pillar is yielding:

- A zone of local yielding in a stress-relieved area,
- A zone of transition from a yielding to the solid state in the pillar, where the stress -concentration area was developed,
- A zone of pillar core that has a uniform confined stress.

The overall pillar stability depends upon the geometrical development of these principal zones. For example, an increase in the yielding pillar area results in a decrease of the solid core, and hence a decrease in its bearing performance, which automatically leads to the instability of the system. Fig. 9 shows the yielding state of the mine structure where the growth of the plastic zone for each load increment is given by the yield Gaussian points. At 50% of the maximum applied load, Fig. 9A, the first plastic zones are shown to occur at the immediate roof-pillar intersection, over the cross-section of the pillar and, to a limited extent, at the floor-pillar intersection. In this case the solid pillar area is over 50% of the total

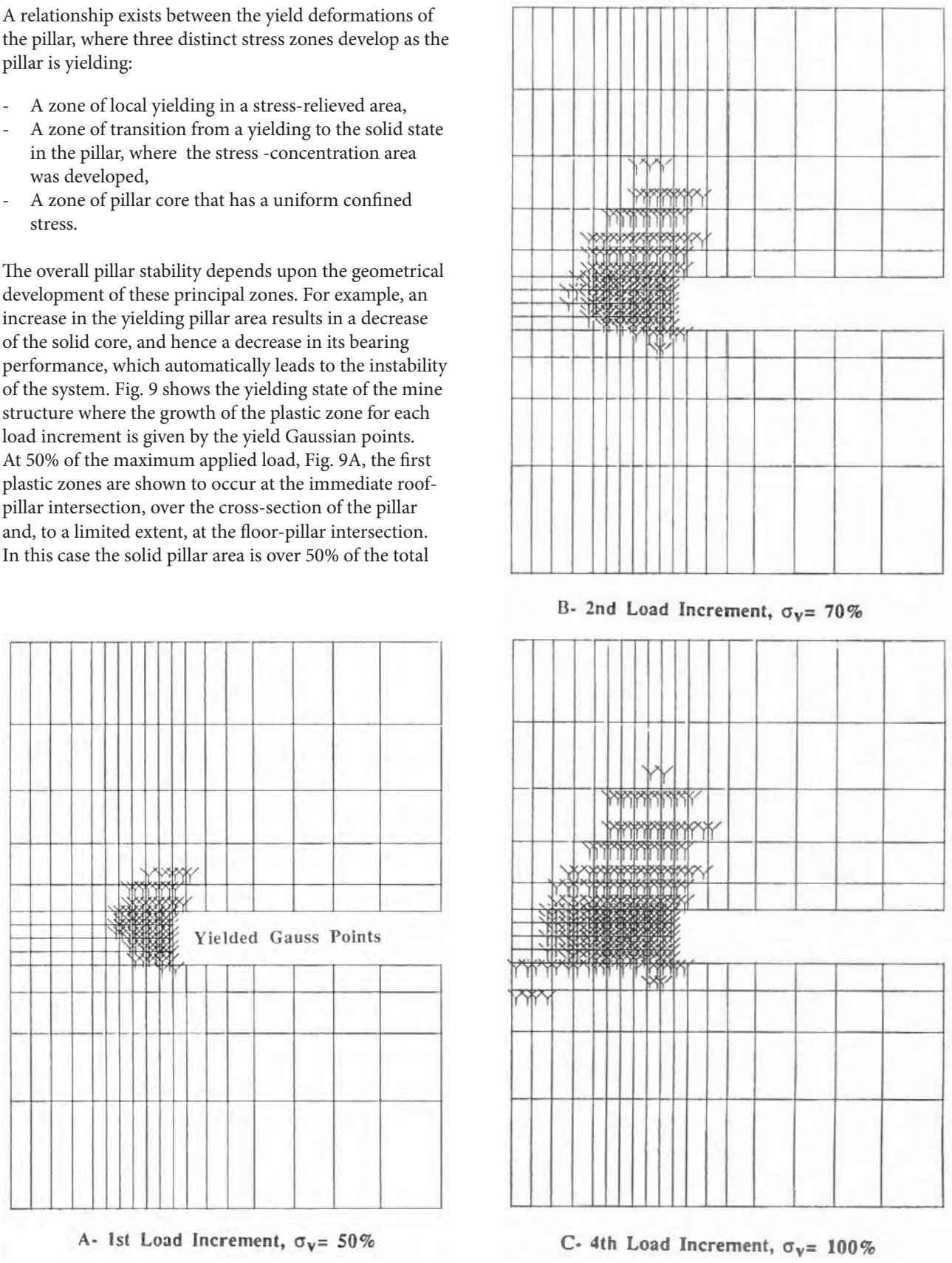

Figure 9. Spread of the yield zone at various applied load levels; the extraction ratio r = 60%.

area, and the pillar is assumed to be stable. As the load is increased, the plastic zone spreads upwards into the immediate roof and laterally into the pillar, Fig. 9B. The effective pillar core is reduced to less than half of the pillar area, but can still provide support. At the final stage of loading, the yielded zone reaches its maximum as the mine structure passes to its final equilibrium steady state, as shown in Fig. 9C, where the plastic zone is seen to increase considerably in both the roof and the pillar, while the floor remains almost unaffected. The effective pillar area is reduced to more than half of the total pillar area and overall pillar instability is likely.

At low extraction ratios of 0.25 and 0.40, as shown in Fig. 10 (A, B), the developed yield zone is confined to an area around the rock-mass opening interface. In both cases the area of effective support is shown to be larger than the outer yield zone. Under these conditions, the pillar is almost at its maximum capability and the mine structure is stable.

The non-linear finite-element analysis was further extended to analyse the influence of the roof, pillar and floor interactions on the overall pillar stability. In order

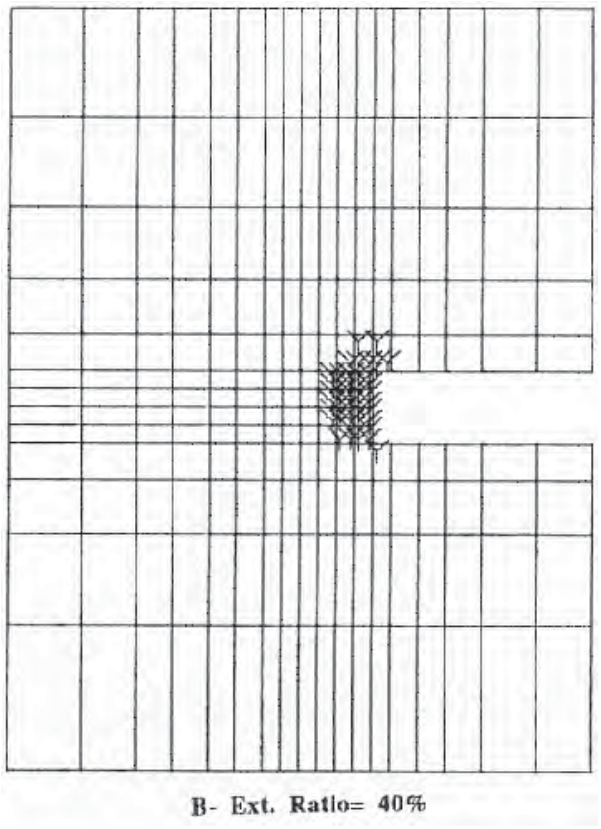

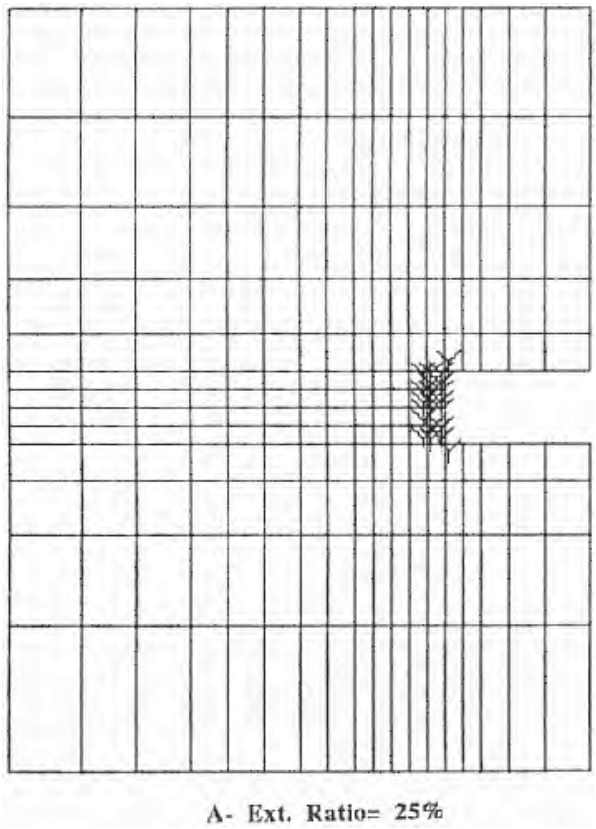

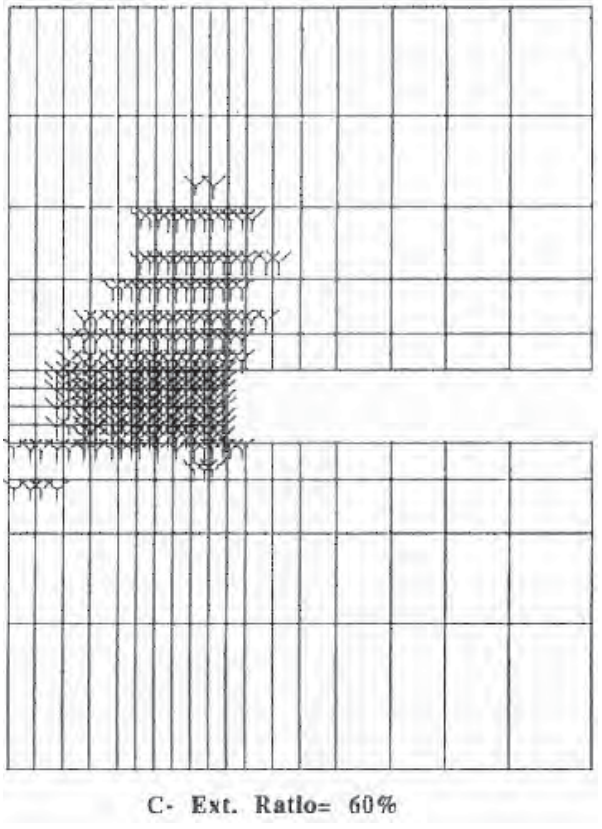

Figure 10. Spread of the yield zone at the full applied load level and various extraction ratios, *r*.

to find out the effect of this interaction as well as the effect of the change of their properties on the overall pillar stability, three models were analysed using different properties for the roof, pillar and floor. Fig. 11 shows the predicted vertical and horizontal stresses of the pillar for model A, having a stiff roof, a weak pillar and a weak floor; and model B, having a weak roof, a weak pillar and a stiff floor; and model C, where the roof and the floor are taken to be stiff and the pillar is kept weak.

It is clear from Fig. 12 (next page) that for the same pillar material in the three suggested models and the different combinations of material properties for the roof and floor, model C shows complete yielding of the pillar, while in model B the area of effective support is considerably reduced, but to a lesser extent than with model C. Finally, in model A, a moderate effective area is indicated in the pillar, which yields to a certain degree. It can be concluded from these findings that the interaction of the roof, pillar and floor has a significant effect on the pillar's overall stability. Therefore, when assessing the stability of a given room and the pillar mine workings, the roof, pillar and floor should be considered as an integrated structure. This approach generally yields more accurate results.

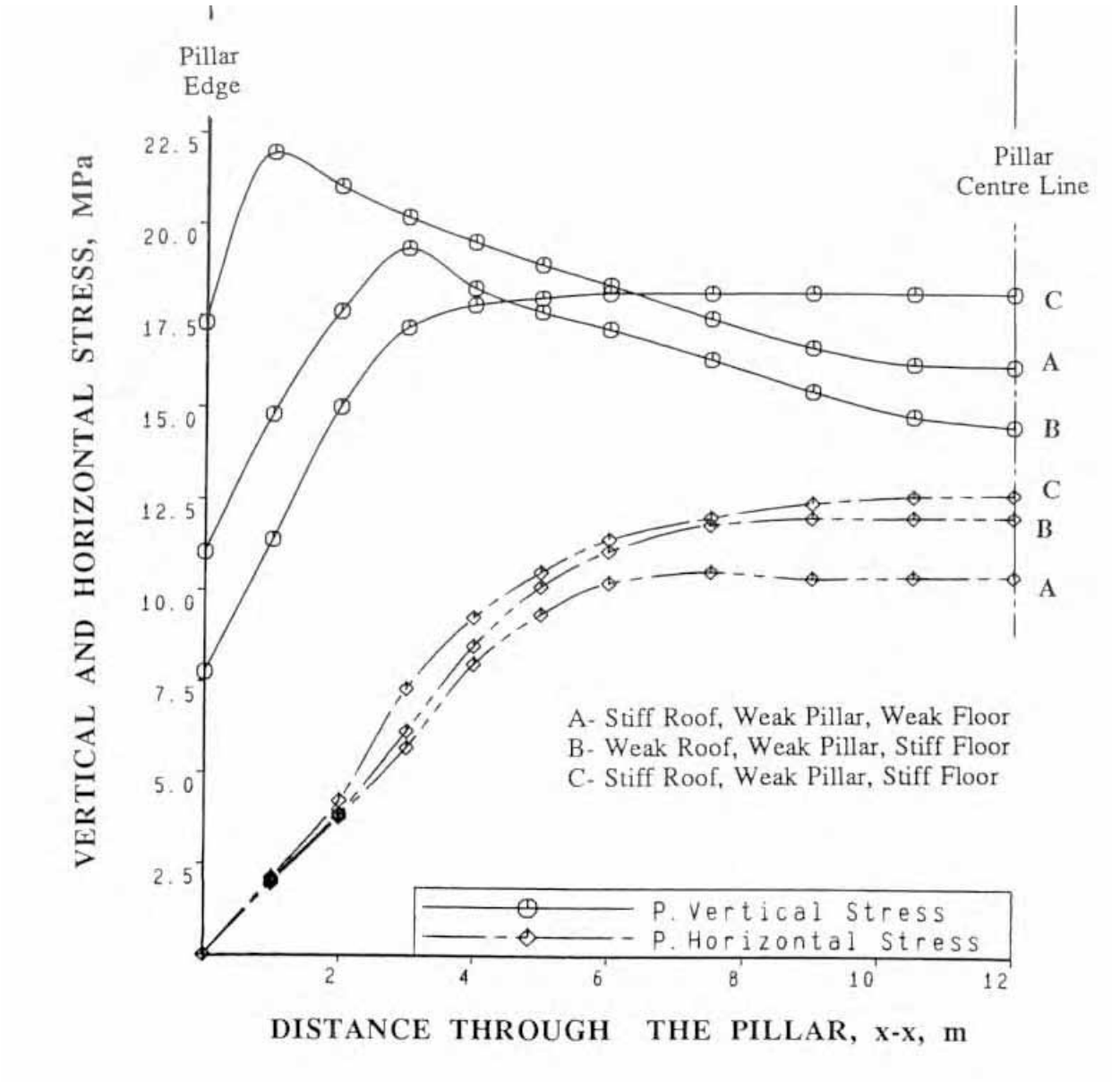

Figure 11. Vertical and horizontal pillar stresses, determined by the elastic-plastic finite-element solution for different models.

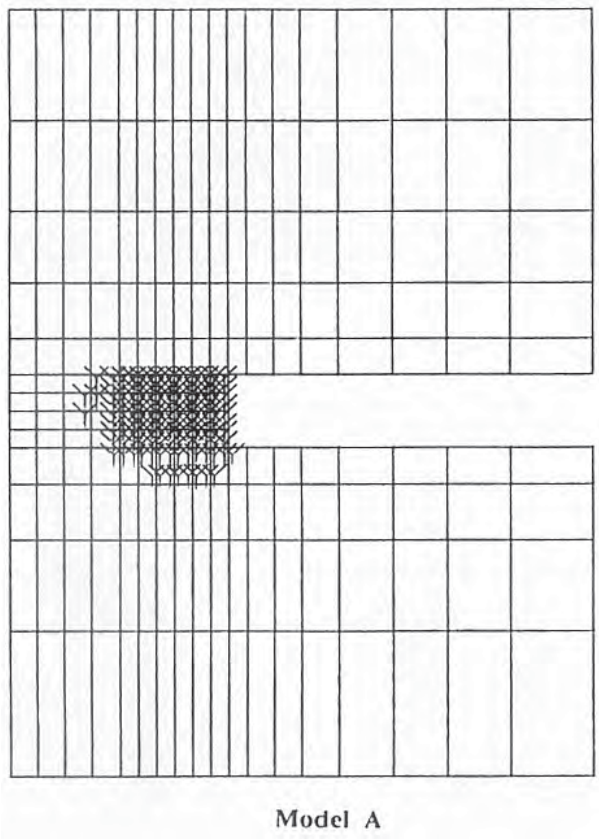

Figure 12. Spread of the yield zone in the mine structure for the three models.

7 CONCLUSION

Based on the modelling results presented above, the following conclusions may be drawn:

- The strain-weakening behaviour of rock layers around a mine opening was simulated using an advanced non-linear elastic-plastic finite-element model, which accounts for the residual strength after failure. This simulation was achieved using a step-by-step iterative computational procedure in which the rock material's stiffness was updated after each run according to the initially applied load, until the solution reached the final equilibrium steady state of the mine structure. The numerical results clearly demonstrate the limitations of the linear model when it comes to realistically representing the overall structure behaviour Fig. 5, particularly when the structure of the rock mass is relatively weak, and that a non-linear approach was justified.
- As progressive mining was simulated in the model, the maximum load in the pillar increased and trans-

ferred laterally towards the centre of the pillar as yielding occurred, this trend of lateral stress transfer and load build up in the core of the pillar is consistent with that observed in situ.

- Based on the simulation results, the upper and lower bounds of the overall room and pillar stability were obtained. Parameters such as the roof, the pillar width, w_p, the extraction height, h_p, the variability of the pillar, roof and floor strength have been shown to significantly affect the mechanism of roof, pillar and floor yield.

REFERENCES

[1] Riks, S.F. (1979). An incremental approach to the solution of snapping and buckling problems. *International Journal of Solid Structure* 15, 29-551.

[2] Nayak, G. C. and Zienkiewicz, O. C. (1972). Elasto-plastic stress analysis. A Generalization for various constitutive relations including strain-softening. *Int. J. Num Meth. Eng*., 5, 113-135.

[3] Zienkiewicz, O. C. Valliappan, S. and King, (1969). Elasto-plastic solutions of engineering problems 'Initial stress' finite element approach. *Int. J. Num. Meth. Eng*.. 1. 75-100.

[4] Crisfield, M. A. (1981). A fast incremental/iterative solution procedure that handles snap-through. *Computers and Structures*, 13, 55-62

[5] Cheng, G. and Karmis, M. (1988). Computer modelling of yield pillar behaviour using post-failure criteria. Proceedings of '88 7th Int. Conf. Ground Control in Mining. West Virginia University, Morgantown, USA.

[6] LUSAS, (1989). Advanced nonlinear finite element analysis.FEA.Ltd, Forge House High street, Kingston upon Thames, Surrey, KTN 1HN.

[7] Park, D. W. and Ash, N. F. (1985). Stability analysis of entries in deep coal mines using finite element method. *Mining Science and Technologie, 3*, 11-20.

[8] Salamon , M.D.G., Badr, S., Mandoza, R., Ozbay, M. U. (2003). Pillar failure in deep coal seems: Numerical simulation. ISRM, 2003 – technology road map for rock mechanics. South Africa.

[9] Colwell, M. G., (1998). Chain pillar design (calibration of ALPS), ACARP research project C6063 Australian coal research Ltd. 66p.

[10] Mark, C. and Barton T. (1996). The uniaxial compressive strength of coal: should it be used to design pillar? *Proceedings of the 14th conference on ground control in mining*, West Virginia University, August 1-3, 63-71.